Scientia Iranica D (2022) 29(3), 1437–1454

Sharif University of Technology
Scientia Iranica
Transactions D: Computer Science & Engineering and Electrical Engineering
http://scientiairanica.sharif.edu

PV/BESS for supporting electric vehicle charging station integration in a capacity-constrained power distribution grid using MCTLBO

K. Kasturi[a,*], M. Ranjan Nayak[b], and C. Kumar Nayak[c]

a. *Department of Electrical Engineering, I.T.E.R., Siksha 'o' Anusandhan University, Bhubaneswar,751030, Odisha, India.*
b. *Department of Electrical Engineering, CAPGS, Biju Patnaik University of Technology, Rourkela, 769015, Odisha, India.*
c. *Department of Electrical Engineering, Indira Gandhi Institute of Technology, Sarang, 759146, Odisha, India.*

Received 4 September 2017; received in revised form 28 November 2019; accepted 8 June 2020

KEYWORDS
Battery Energy Storage System (BESS);
Photovoltaic (PV);
Charging Station (CS);
Radial Distribution System (RDS);
Multi-Course Teaching Learning-Based multi-objective Optimization (MCTLBO).

Abstract. Solar Photovoltaic (PV) systems with a back-up Battery Energy Storage System (BESS) mitigate power system-related issues including ever-increasing load demand, power loss, voltage deviation, and need for power system upgradation as the integration of Electric Vehicles (EVs) increases load while charging. This paper investigates the improvements of system parameters such as voltage, power loss, and loading capabilities of IEEE-69 bus Radial Distribution System (RDS) with PV/BESS-powered EV Charging Stations (CSs). The RDS is divided into different zones depending on the total number of EVs, EV charging time, and available CS service time. One CS is assigned to each zone. An energy management strategy is developed to direct the power flow among the CS, PV panel, BESS, and the utility grid according to time of use of electricity price. The BESS is allowed to sell excess energy stored to the utility grid during peak hours. Multi-Course Teaching Learning-Based multi-objective Optimization (MCTLBO) is used to optimize the size of PV/BESS system and the locations of CSs in each zone to minimize both the annual CS operating cost and the system active power loss. The results validate the proper function of optimal PV/BESS to power CS for techno-economic improvement of the system.

1. Introduction

1.1. Motivation

Advances in technologies related to Electric Vehicles (EVs) and use of renewable energy sources, such as solar photovoltaic (PV) cells, are quite evident in power distribution systems worldwide. EVs are gaining popularity quickly over Internal Combustion Engine (ICE) powered vehicles due to their environment-friendliness, unlike ICE-operated vehicles [1-3]. Another advantage of EVs is the drastic fall in fuel cost, i.e., recharging of EVs by electricity is cheaper than the petroleum fuel ICE use. The major disadvantage of EV is the need for recharging its battery at Charging Stations (CS) at regular intervals [4]. However, high load current requirement of CSs increases the transmission loss of the grid immensely. Therefore, using PV panels to assist the utility grid in supplying power to the CS is both economically and technically viable [5]. However, the unpredictable nature of solar radiation adversely affects power system reliability. The system reliability can effectively be enhanced by using Battery Energy Storage System (BESS). Addition of new energy producers (PV and BESS discharging) and

*. *Corresponding author.*
E-mail address: kumari.kasturi1986@gmail.com (K. Kasturi)

doi: 10.24200/sci.2020.5128.1112

energy consumers (EV and BESS charging) affects the network performance either positively or negatively. The consequences of this fact depend on many aspects such as the place where the generation or the load is added and the quantity of power transactions involved. It is utterly important for the CS planner to analyze the ability of the network to accept new production or load by optimizing the location of CS (keeping an eye on traffic conditions) and size of PV and BESS to lessen its adverse impact on the distribution grid [6].

1.2. Literature survey

Optimal planning of CSs with renewable resources as well as its impact on the connected distribution grid are the emerging areas of research [7]. Different methods have been adopted to determine the optimal allocation of CSs to keep the voltage and line loading limits of the distribution system within acceptable thresholds. Another factor to consider for EV is city traffic networks on their way to CSs for charging. In [8], a Multi-Objective Hybrid Ant Colony Optimization and Bees Algorithm (MOHACOBA) was used to optimize the placement of Fast Charging Stations (FCS) to cut down real power loss in the feeders of IEEE-69 bus Radial Distribution System (RDS). The approach was more biased towards comparing different optimization techniques and proving the superiority of the proposed MOHACOBA by evaluating different performance matrices. In [9], a Modified Primal-Dual Interior Point Algorithm (MPDIPA) was used to solve the problem of optimal sizing of EVCSs whose locations were previously identified via a screening method. Here, the objective was to reduce the network loss and enhance the system voltage. However, Renewable Energy Sources (RES) were excluded to further improve the system parameters such as power loss and voltage. In [10], an analytical method was employed in conjunction with the sequential placement approach to determine the placement of Distributed Generators (DGs) and CS in the IEEE-33 bus RDS. Here, the objective was to reduce the system power loss. This paper considered the economic benefits of neither utility grid nor EV owners. In [11], the authors used Differential Evolution (DE) algorithm to optimize the location and size of EVCSs and RES such as solar PV and wind energy, respectively. The objective function in this paper was formulated as the weighted sum of active power loss, total voltage profile index, and electricity costs related to EV charging and load supply. This paper discussed the impact of integration of a large number of EVs into a distribution network. The benefits of using BES system under Time Of Use (TOU) pricing were based on the optimal battery size [12]. In [13], a non-linear programming problem was formulated using two objectives of minimizing the Total Annual Energy Losses (TAEL) and the Cost Of Energy (COE) for a microgrid with DG and storage. Sequential quadratic programming was employed to solve the problem for both grid-connected and stand-alone modes of operation. The results ensured a significant reduction in TAEL and COE and a remarkably higher degree of independence from the utility grid. In [14], a two-stage approach to the allocation of EV parking lot and DERs in a distribution network was proposed. Selection of an appropriate bus for EV parking based on economic objectives was performed, followed by allocation of DERs and EV parking lot to reduce the distribution system loss using Genetic Algorithm (GA) and Particle Swarm Optimization (PSO) algorithm. The results validated the superiority of simultaneous allocation of DERs and EV parking lots over the approach of independent allocation. In [15], the game theory was employed to design a practical demand response program for optimal charging schedule of PHEVs subjected to the minimization of customers' charging cost. The proposed algorithm was compatible with dynamic pricing. The results showed that the proposed method was successful in producing outcomes of immense utility for PHEV charging scheduling. In [16], the GA-PSO hybrid improved optimization algorithm was used to optimize an objective function that was formulated by combining power losses, voltage fluctuations, charging and electricity costs, and EV battery cost. This paper presented optimal planning of RES powered CSs in a distribution network taking into account two perspectives of (i) the system operator and (ii) customers and EV owners. In [17], a decentralized decision-making algorithm was presented for optimal power flow in a collaboration between transmission and distribution system operators. Here, the co-ordination strategies among the two power system operators were strengthened without the help of a central co-ordinator keeping their information private. In [18], the problem of a rise in load demand due to PHEV charging was posed as a non-cooperative game theory problem with an eye on optimizing the costs borne by the utility companies and the customers. A distributed algorithm was developed to ensure its convergence to the unique Nash equilibrium from any arbitrary initial conditions. The existence of a Lyapunov's function was well established. In order to reschedule the consumers' energy usage to off-peak hours, an actor-critic based online load scheduling learning algorithm was developed in [19]. The users' load scheduling policy was approximated using Markov's perfect equilibrium. The simulation results observed a significant reduction at peak-to-average demand ratio and the burden of costs on the users.

1.3. Contributions

In contrast to prior studies, this paper follows the approach of dividing the total distribution network

into 6 zones depending on the total number of EVs, time taken by each EV to charge completely, and the available service time of each CS. Each zone is assigned to one CS and traffic networks are considered to direct EVs to the nearest CS for charging purpose. Two-level time-of-use pricing is employed to determine the power flow among CS, EVs, PV panels, BESS, and utility grid. Here, the back-up BESS is allowed to sell power to the utility grid when the electricity price is higher. It enables the distribution system operator to obtain financial benefits and to shed a significant part of peak load demand off the utility grid's responsibility. Apart from this, unique and efficient modifications made to the well-known Teaching Learning Based Optimization (TLBO) technique are addressed and utilized. Unlike the traditional TLBO, additional two phases namely teachers' training and exchange students' phases have been introduced to fasten the convergence and generate a more accurate output. The optimization results are compared with those obtained from Non-dominated Sorting Genetic Algorithm-II (NSGA-II).

1.4. Organization of the paper

An overview of the configuration of the proposed system model including the PV system, BESS, and load profile as well as the modeling of charging stations are briefed in Section 2. Section 3 discusses the strategy adopted for energy management in the proposed system model. The problem under investigation is formulated mathematically in Section 4. The evolutionary optimization technique, Multi-Course Teaching Learning-Based multi-objective Optimization (MCTLBO) and its application to the problem under investigations are discussed in Section 5. Before concluding the paper in Section 7, the contribution is validated by presenting and analyzing the simulation results in Section 6.

2. Modeling of the system

Figure 1 presents the system configuration and power transaction among the components CS with PV and BESS. The CS, PV, BESS, grid, and load were connected to a common AC bus bar. The DC output power of the PV panel is converted into AC with the help of a PV inverter so that it can be fed to the AC bus. To facilitate bi-directional power transaction among the BESS and AC bus, an inverter/charger unit was used [20]. One CS contains 5 Charging Circuits (CC). The PV, BESS, and CS are connected to the RDS at the ith load bus. The 24-hour load demand is assumed to follow the IEEE reliability test system load profile [21,2] and a lagging power factor of 0.9 is considered. The loads with CS, PV, and BESS are distributed equally at each phase on load bus. Backward and forward sweep-based algorithm has been used for distribution system load flow analysis [22,2] due to its high computational efficiency with robust convergence characteristic.

2.1. Modeling of the PV system

The PV power of DC nature is directly proportional to the global horizontal irradiation and the PV cell efficiency in a standard temperature condition. How-

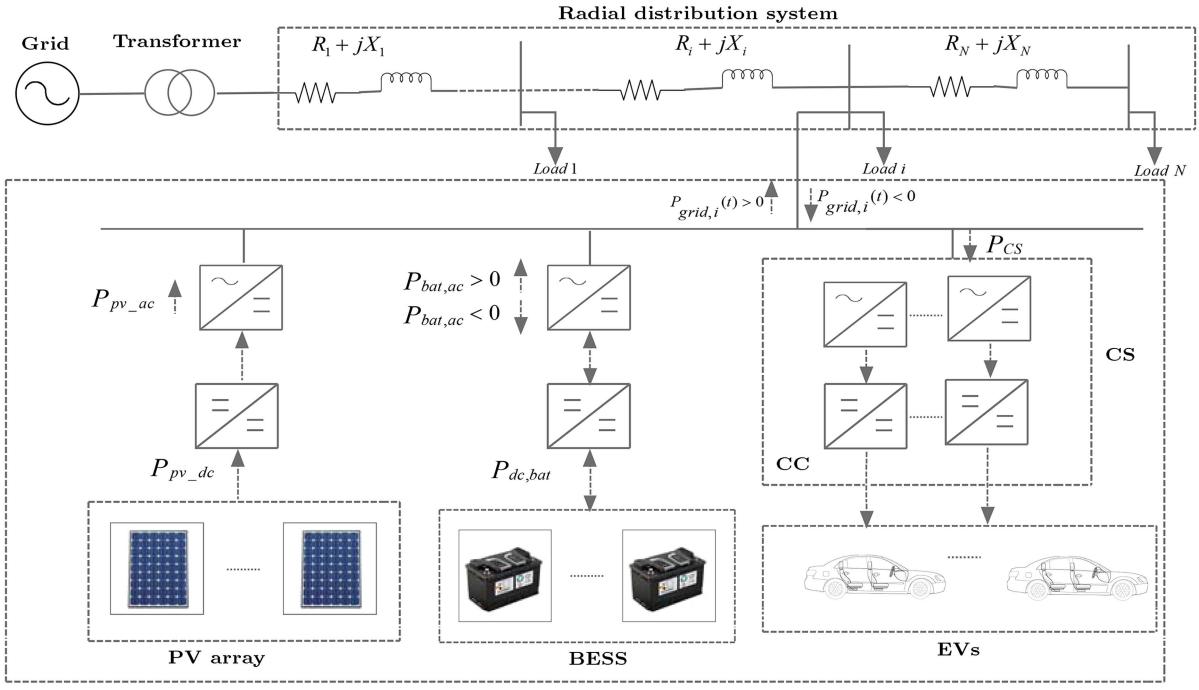

Figure 1. Charging station with PV and BESS.

ever, the efficiency is greatly affected and de-rated by factors like variation of temperature, manufacturer's limitations, deposition of dirt and dust on the panel, and losses incurred along the cable and during the switching instances [20,23–24].

$$P_{pv\_dc}(t) = A_{pv} \times \eta_{pv} \times \eta_{pt} \times I(t) \times N_{pv} \times f_{man} \times f_{dirt} \times f_{cell} \times \eta_{pv\_inv}. \quad (1)$$

The power rating of each PV panel is 5 kW_p. The derating factor due to temperature (f_{cell}) can be calculated as follows:

$$f_{cell} = [1 - T_{co} \times (T_m - T_{ref})]. \quad (2)$$

The module temperature (T_m) is calculated as follows [20,25]:

$$T_m = T_{amb} + (\frac{NOC - 20}{800}) \times I(t). \quad (3)$$

The AC power output at the AC bus bar is calculated as follows:

$$P_{pv\_ac}(t) = P_{pv\_dc}(t) \times \eta_{inv} \times \eta_{inv\_sb}. \quad (4)$$

Solar radiation data for Bhubaneswar for the year 2015 are collected from the Indian Meteorological Department [20,26]. Hourly average solar radiation data along with load weight factors are shown in Figure 2.

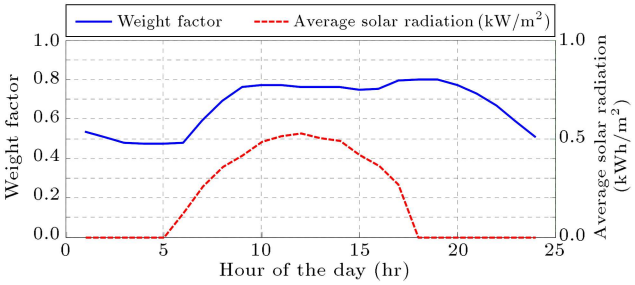

Figure 2. Average hourly solar radiation and hourly weight factor in a day.

2.2. Modelling of BESS

In this system, valve-regulated, sealed gelled electrolyte lead-acid batteries were used because their lifespan will not be weakened if subjected to frequent charging and discharging [20].

Maximum capacity of the battery can be calculated as follows [27–29]:

$$C_{\max} = 1.67 * C * (1 + 0.005 * (T_{amb} - 25)). \quad (5)$$

The capacity of the BESS at hour t can be calculated as:

$$C_{bat}(t) = \frac{C_{\max}}{1 + 0.67\left(\frac{I_b(t)}{I_{rate}}\right)^{0.9}}. \quad (6)$$

The State Of Charge (SOC) and the battery cell voltage (V_b) are updated every hour [20]. These are calculated in relation to its previous value taken at hour $t-1$.

During peak hours (BESS discharging), we have:

$$SOC(t) = \begin{cases} SOC(t-1) & SOC(t) \le SOC^{\min} \\ SOC(t-1) + \left(\frac{I_b(t)}{C_{bat}(t)}\right) & SOC(t) > SOC^{\min} \end{cases} \quad (7)$$

$V_b(t)$ is calculated by Eq. (8) as shown in Box I.

During off-peak hours (BESS charging), we have:

$$SOC(t) = \begin{cases} SOC(t-1) & SOC(t) \ge SOC^{\max} \\ SOC(t-1) + \left(\frac{I_b(t)}{C_{bat}(t)}\right) & SOC(t) < SOC^{\max} \end{cases} \quad (9)$$

In this regard $V_b(t)$ is calculated by Eq. (10) as shown in Box II. The battery cell voltage has been approximated using Eqs. (8) and (10) [30].

Charging or discharging rate of the BESS can be calculated as follows [31]:

$$P_{dc,bat}(t) = E_{bat}(t) - E_{bat}(t-1). \quad (11)$$

The BESS power output at the AC bus bar is calculated as follows:

$$P_{bat,ac}(t) = P_{dc,bat}(t) \times \eta_{inv} \times \eta_{inv\_sb}. \quad (12)$$

The details of battery specifications used as variables for optimization of the energy schedule are given in Table 1 [20].

$$V_b(t) = \begin{cases} V_b(t-1) & SOC\ (t) \le SOC^{\min} \\ n_b\,[1.965 + 0.12\ SOC\ (t)] - n_b\ \frac{|I_b(t)|}{C}\left(\frac{4}{1+|I_b(t)|^{1.3}} + \frac{0.27}{SOC\ (t)^{1.5}} + 0.02\right)(1 - 0.007\ \Delta T) & SOC\ (t) > SOC^{\min} \end{cases} \quad (8)$$

Box I

$$V_b(t) = \begin{cases} V_b(t-1) & SOC\ (t) \geq SOC^{\max} \\ n_b\left[2 + 0.16\ SOC\ (t)\right] - n_b \frac{|I_b(t)|}{C}\left(\frac{4}{1+\ |I_b(t)|^{\ 1.3}} + \frac{0.27}{SOC\quad(t)^{1.5}} + 0.02\right)(1 - 0.007\Delta T) & \\ & SOC\ (t) < SOC^{\max} \end{cases} \quad (10)$$

Box II

Table 1. Battery specifications [20,32,33].

Name of the Parameter	Specification
Individual battery capacity	1500Ah
Nominal battery voltage	12V
Initial battery voltage	12.5V
Minimum state of charge ($SOC^{\min}$)	30%
Maximum state of charge ($SOC^{\max}$)	90%
Minimum charging/discharging time ($t_{\min}$)	10 h
Charge or discharge current in 10h at 25°C (I_{rate})	150A

2.3. Modelling of the load and CS

The predicted load demand of RDS & CS at bus i at any desired time t can be calculated as follows [2]:

$$P_{Load,i}(t) = w_h(t) \times P_i, \quad (13)$$

$$P_{CS,i}(t) = w_h(t) \times C_{CS,i}. \quad (14)$$

As shown in Figure 2, $w_h(t)$ is the hourly weight factors used for modeling the load demand of RDS and CSs in 24 hours [22,2].

Each CS is set up to 440 Volt, 227 Amp, 50 Hz, and 100 kVA. The number of required CSs in the 69-bus RDS can be calculated as follows [2]:

$$n^{CS} = \left[\frac{NEV \times chg_{time}}{s_h \times q}\right] + 1. \quad (15)$$

Rounding n^{CS} to its nearest integer value helps achieve the number of CSs required for the distribution network.

3. Energy management strategy

A total of four scenarios constitute the whole operation strategy [31]:

- **Scenario 1.** $[P_{pv-ac}(t) + P_{bat,ac}(t) > P_{CS}(t)]$ and during peak hours of the day: Net PV power is sold to the grid as the cost is higher during peak hour. If the SOC of BESS is greater than $SOC^{\min}$, then the BESS is also allowed to discharge to sell power to the grid. Otherwise, the BESS remains idle;
- **Scenario 2.** $[P_{pv-ac}(t) + P_{bat,ac}(t) < P_{CS}(t)]$ and during peak hours of the day: The BESS discharges to supply the CS if SOC of BESS is more than $SOC^{\min}$. If the net requirement of CS is less than the maximum discharging rate of the BESS, the BESS will discharge at the required rate to meet the need of CS. The remaining energy stored in the BESS will be sold to the grid. Otherwise, BESS will discharge at its maximum rate to supply the CS. If PV and BESS are unable to meet the requirement of CS, then the CS will be fed by the grid;
- **Scenario 3.** $[P_{pv-ac}(t) + P_{bat,ac}(t) > P_{CS}(t)]$ and during off-peak hours of the day: The net PV power will charge the BESS provided that its SOC is less than $SCO^{\max}$. In this case, if the net PV power is less than the maximum charging rate of the BESS, then the BESS charges with the net generated power. Otherwise, it will charge at its maximum rate. If the BESS is at its $SCO^{\max}$, then the net generated PV power will be sold to the grid;
- **Scenario 4.** $[P_{pv-ac}(t) + P_{bat,ac}(t) < P_{CS}(t)]$ and during off-peak hours of the day: In this scenario, the CS is fed by the utility grid only. The BESS is not allowed to discharge during this period. Because if the excess stored energy is sold to the grid during peak hours, better economic profitability is achieved.

During peak hour of the day:

$$P_{grid}\ (t) = P_{Load}\ (t)\ -\ (P_{pv\_ac}\ (t)\ -\ P^{ch}_{bat\,,ac}(t) - P_{CS}(t)\ ), \quad (16)$$

$$Q_{grid}\ \ (t) = P_{grid}(t) \times \tan(\cos^{-1}(pf)). \quad (17)$$

During off-peak hours of the day:

Table 2. TOU rates for electricity.

	Peak Periods (7 a.m. – 1 p.m. & 4 p.m. –10 p.m.)	Off-Peak periods (1 p.m. – 4 p.m. & 10 p.m.–7 a.m.)
Electricity price (INR/kWh)	6.00	4.00

$$P_{grid}\ (t) = P_{Load}\ (t)\ -\ (P_{pv\_ac}\ (t) + P^{disch}_{bat,\ ac}\ (t) - P_{CS}\ (t)\ ), \tag{18}$$

$$Q_{grid}\ (t) = P_{grid}(t) \times \tan(\cos^{-1}(pf)). \tag{19}$$

4. Problem formulation

The proposed MCTLBO model is developed as a multi-objective and multi-period minimization model that is carried out within the framework of the nonlinear constraints [20]. The main objective is to determine the optimal sites where PV/BESS integrated CS should be located. The multi-objective approach of the proposed MCTLBO serves two objectives of minimizing the total annual cost of the system ($f_{obj,1}$) and the total annual power loss ($f_{obj,2}$) in the distribution system [2].

4.1. Objective Functions

4.1.1. Total annual cost of CSs with PV and BESS ($f_{obj,1}$)

The total annual cost of CSs with PV and BESS can be calculated as follows:

$$f_{obj,1} = C_{CS} + C_{PV\&BESS}, \tag{20}$$

$$C_{CS} = C^{CS}_{INV} + C^{CS}_{O\&M} + C^{CS}_{TRV} + C^{CS}_{ele}, \tag{21}$$

$$C^{CS}_{INV} = \sum_{o=1}^{n^{CS}} U^{CS}_{INV} \left[\frac{ir\,(1+ir)^e}{(1+ir)^e - 1}\right], \tag{22}$$

$$C^{CS}_{O\&M} = \sum_{o=1}^{n^{CS}} \sigma\, U^{CS}_{INV}, \tag{23}$$

$$C^{CS}_{TRV} = x\varsigma\eta\kappa\, l \sum_{p=1}^{lp}\sum_{o=1}^{n^{CS}} g^{ph}\, d^{ph}, \tag{24}$$

$$C^{CS}_{ele} = E_{price}(t) \times E_{grid}(t). \tag{25}$$

Annual investment cost (C^{CS}_{INV}) is used to calculate the total capital recovery cost of CS [2]. Annual operational and maintenance costs of CS ($C^{CS}_{O\&M}$) include material cost, staff salary, maintenance and operation cost, and power consumption cost [2]. Travelling cost of EVs (C^{CS}_{TRV}) reflects the costs incurred by transport of EVs to CSs to recharge the battery for a whole year. Negative and positive values of $E_{grid}(t)$ signify the acts of purchasing and selling electricity from and to the utility grid, respectively. The prices of electrical energy are set based on time of use, as shown in Table 2. The selling and purchasing prices of electricity are assumed to be the same. g^{ph} is calculated as [2]:

$$g^{ph} = \begin{cases} 1 & d^{ph} \le d^{\max} \\ 0 & else \end{cases} \tag{26}$$

The distance between CS and load point is collected as follows [2,34]:

$$C_{PV\&BESS} = f^{PV\&BESS}_{INV} + f^{PV\&BESS}_{O\&M}, \tag{27}$$

$$f^{PV\&BESS}_{INV} = \sum_{o=1}^{n^{PV\&BESS}} U^{PV\&BESS}_{INV} \left[\frac{ir\,(1+ir)^e}{(1+ir)^e - 1}\right], \tag{28}$$

$$f^{PV\&BESS}_{O\&M} = \sum_{o=1}^{n^{PV\&BESS}} \sigma\, U^{PV\&BESS}_{INV}, \tag{29}$$

$U^{PV\&BESS}_{INV}$ includes the investment cost of the BESS = INR 5500 per kWh, the investment cost of the inverter = INR 6000 per kW, and the investment cost of the PV panels = INR 35 per W_p [2].

4.1.2. Total annual Power Loss ($f_{obj,2}$)

Total power loss can be calculated for one year (8760 hours) as follows:

$$f_{obj,2} = \sum_{h=1}^{8760}\sum_{ij=1}^{i-1} P_{Loss\ ,ij}(t), \tag{30}$$

$$P_{Loss,\,ij}(t) = R_{ij} I^2_{ij}(t). \tag{31}$$

4.2. System operational constraints

The solution of the optimization problem considers the following constraints:

$$P_{sub}(t) \pm P_{grid}(t) = P_{Load}(t) + P_{Loss}(t), \tag{32}$$

$$Q_{sub}(t) \pm Q_{grid}(t) = Q_{Load}(t) + Q_{Loss}(t), \tag{33}$$

$$V^{\min}_i \le V_i(t) \le V^{\max}_i, \tag{34}$$

$$I_{ij}(t) \le I^{\max}_{ij}, \tag{35}$$

$$P^{\min}_{pv\_dc} \le P_{pv\_dc}(t) \le P^{\max}_{pv\_dc}, \tag{36}$$

$$P_{dc,bat}^{\min} \leq P_{dc,bat}(t) \leq P_{dc,bat}^{\max}, \quad (37)$$

$$SOC^{\min} \leq SOC(t) \leq SOC^{\max}, \quad (38)$$

$$P_{EV}^{\min} \leq P_{EV}(t) \leq P_{EV}^{\max}, \quad (39)$$

$$P_{CS} \leq P_{CS}^{\max}, \quad (40)$$

$$P_h chg_{time} \sum_{p=1}^{lp} n_{EV}^{p} g^{ph} \leq \sum_{t=1}^{n_t} \sum_{k=1}^{n^{CS}} P_{CS}^{\max} s_h w_h(t), \quad (41)$$

$$d_{CS}^{\min} \leq d_{CS}(t) \leq d_{CS}^{\max}, \quad (42)$$

$$\sum_{p=1}^{lp} \sum_{o=1}^{n^{CS}} g^{ph} \geq lp, \quad (43)$$

where positive and negative signs are used for delivering power to the grid and consuming power from it, respectively.

4.3. Charging stations cost benefit

The cost benefits of installing CSs with PV and BESS are computed as follows:

$$B_{CS} = \sum_{k=1}^{n^{CS}} [C_{grid,CS} - (C_{grid,CS}^{PV\&BESS} - C_{grid,PV\&BESS}^{CS})] - C_{PV\&BESS}, \quad (44)$$

$$C_{grid,CS} = [E_{price}(t) \times E_{grid,CS}(t)] \times 365, \quad (45)$$

$$C_{grid,CS}^{PV\&BESS} = [E_{price}(t) \times E_{grid,CS}^{PV\&BESS}(t)] \times 365, \quad (46)$$

$$C_{grid,PV\&BESS}^{CS} = [E_{price}(t) \times E_{grid,PV\&BESS}^{CS}(t)] \times 365. \quad (47)$$

After meeting the objectives of the optimization program, Voltage Stability Index (VSI), an indicator of the health of the distribution network, is evaluated. The VSI at bus j is calculated as follows:

$$VSI = \frac{1}{24} \times \sum_{t=1}^{24} [|V_i(t)|^4 - 4\left[P_j(t) \cdot X_{ij} - Q_j(t) \cdot R_{ij}\right]^2 - 4[P_j(t) \cdot R_{ij} + Q_j(t) \cdot X_{ij}] |V_i(t)|^2]^{-1}, \quad (48)$$

where i and j are the sending end and the receiving end buses, respectively. To ensure a stable operation, VSI must be minimum and greater than zero. Buses with maximum VSI are unstable. Hence, it is of paramount importance to identify the weak buses and to minimize the VSI of the weakest bus to ensure the system voltage stability.

5. Multi-course teaching learning based multi-objective optimization algorithm

5.1. Multi-objective optimization

The general expression of the multi-objective problem is given as [35]:

$$\begin{aligned} &\min F(x) = (f_1(x), f_2(x), ..., f_w(x)) \\ &x \in S \\ &x = (x_1, x_2, ..., x_n), \end{aligned} \quad (49)$$

where $f_1(x), f_2(x), ..., f_3(x)$ are the w objective functions, $(x_1, x_2, ..., x_n)$ are the n optimization parameters, and $S \in R^n$ is the solution and parameter space [20]. In the multi-objective algorithms, all of the objective functions can be optimized simultaneously with the help of Pareto optimal solution. The solution x is said to dominate y (denoted by $x \succ y$) when the following condition is satisfied [36]:

$$\forall i \in 1, 2, ..., k | f_i(x) \leq f_i(y) \wedge \exists j \in 1, 2, ..., k | f_j(x) \langle f_j(y). \quad (50)$$

When x and y do not dominate each other, they are said to be Pareto-equivalent to each other. The true Pareto-optimal set is a set of solutions that are Pareto-equivalent to each other and cannot be dominated by any other solutions in S. In a Multi-Objective optimization Problem (MOP), the optimization aims to find the entire set or subsets of all non-dominated solutions, known as true Pareto optimal set.

5.2. Teaching Learning-Based Optimization (TLBO)

The basic TLBO was first suggested by Rao et al. [37]. The meta-heuristic evolutionary algorithm is based on teaching and learning activities in a class room [20,38–40]. Two phases of TLBO technique are the "teacher phase" and the "learner phase". Evolutionary population is considered as a class of students, and the best student among the class is selected as the teacher. Students learn from their teacher at the teacher phase and then, learn through interactions with their peers at the learner phase.

5.3. Multi-course TLBO

The basic TLBO has been subjected to modifications in order to solve multi-objective problems in this paper. This modified version includes four phases that are discussed below:

(a) *Formulation of non-dominated set.* Non-dominated set of solutions is obtained by disposing the dominated solutions with the help of a fast-sorting technique that identifies the first non-dominated front. This technique lowers the computational complexity to a significant extent. Initially, the

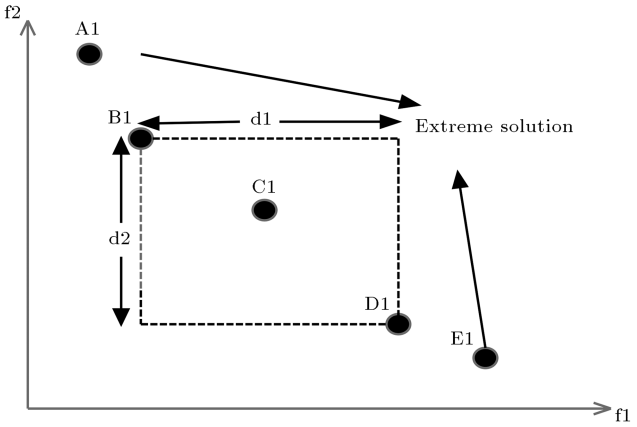

Figure 3. An example of crowding distance calculation [20,39,40].

size of the non-dominated set is assigned to zero. Among the population, for each solution $\bar{X}_i$, the following steps are applied:

- If the non-dominated set is an empty set, $\bar{X}_i$ is added into the set [35];
- Otherwise, the dominance of $\bar{X}_i$ over $\bar{X}_j$ is investigated. If $\bar{X}_i$ dominates $\bar{X}_j$, then $\bar{X}_j$ is rejected. If $\bar{X}_i$ cannot be dominated by any solution in the non-dominated set, then it is added to the set.

Extreme solutions are assumed to have either the maximum or minimum function values. Figure 3 illustrates the calculation of crowding distance for an optimization problem with two objective functions. The solutions that are not dominated by any other solutions are shown as dots in the figure. Here, A1 and E1 are the extreme solutions representing the maximum f2, minimum f1, maximum f1, and minimum f2, respectively. For all the other intermediate solutions, the crowding distance i_{dis} can be calculated by summing up the differences in the position of their neighbouring solutions. For C1, the crowding distance, here, is d1 plus d2 [20].

(b) *Teacher phase.* In general, one teacher is required to teach one basic course to students. While taking teaching learning process as the basis of an MOP, different courses are considered analogous to different objective functions and marks obtained in the courses hold the analogy to their function values. Solution with the best function values of the ith objective located at the extreme position is regarded as the teacher of the ith course. Apart from that, solutions that have the largest crowding distance than other solutions in the non-dominated set are regarded as teachers. It is done so to ensure the melange of population and solutions' improvement. Introduction of more teachers marks a very important improvement of MCTLBO. Solutions other than the selected teacher solutions in the population are improved simultaneously.

Tuning of any influential parameters is not indispensable in case of basic TLBO, which makes the technique a simpler optimization tool. However, teacher count should be taken into account and tuned appropriately in MCTLBO [20].

Unlike the basic TLBO, the modified version distributes students' learning capabilities in the range of 0% to 100% [20]. Thus, the teaching factor is distributed in [0, 1] which significantly improves the convergence and exploration of the algorithm. A very large teaching factor accelerates the convergence process; however, at the same time, it inhibits the exploration capability of the algorithm. The teaching factor is calculated as follows:

$$T_F = \frac{M_i}{M_{new}} = \begin{cases} 2 & if \quad T_F > 2 \\ T_F & if \quad 1 \leq T_F \geq 2 \\ 1 & if \quad T_F < 1 \end{cases} \tag{51}$$

Thus, the teaching factor quantifies the influence of teachers on students and inherently adjusts itself.

(c) *Teacher training phase.* In the non-dominated set, the rest of solutions are considered as candidate trainers [35]. Each teacher T_i improves the performance from a randomly selected trainer. T_i is updated as follows:

$$T_{new,i} = T_{old,i} + r_i \times (T_{trainer} - T_i). \tag{52}$$

A selection operator is introduced to select a solution from $T_{new,i}$ and $T_{old,i}$ [20]. If $T_{new,i}$ is a better solution than $T_{old,i}$, a new one is included and $T_{old,i}$ is rejected. To ensure non-dominance on each other, a simple random approach of tossing a coin is adopted to choose the accepted solution. Figure 4 illustrates the process of determining the selection operator.

(d) *Exchange student phase.* Exchange students from an alien school as well as local students can improve themselves by interactions among them. This phase introduces a mutation operator that includes an exchange student into the current class by randomly selecting three solutions from the non-dominated set [20].

Let $\bar{X}_1$, $\bar{X}_2$, and $\bar{X}_3$ be the solutions chosen by the mutation operator. Now, the mutation process is performed as follows [35]:

$$R = \left|f(\bar{X}_1)\right| + \left|f(\bar{X}_2)\right| + \left|f(\bar{X}_3)\right|, \tag{53}$$

$$R_1 = \frac{\left|f(\bar{X}_1)\right|}{R}, \tag{54}$$

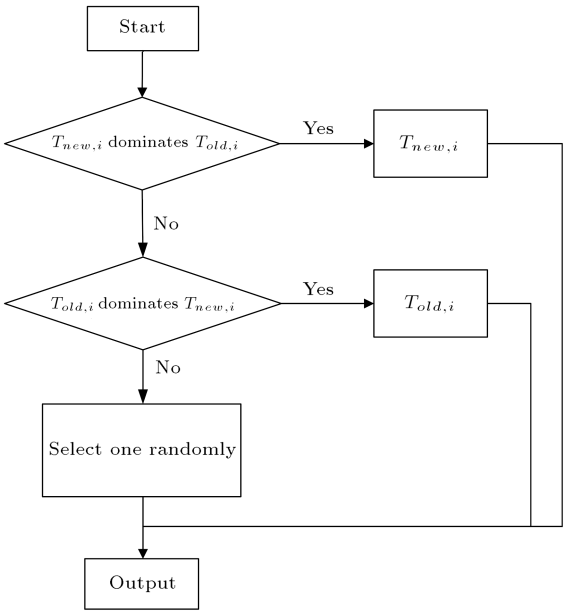

Figure 4. The process of selection operator [20].

$$R_2 = \frac{\left|f(\bar{X}_2)\right|}{R}, \tag{55}$$

$$R_3 = \frac{\left|f(\bar{X}_3)\right|}{R}, \tag{56}$$

$$X_{exchange} = \left(\frac{\bar{X}_1 + \bar{X}_2 + \bar{X}_3}{3}\right) + (R_1 - R_2) \left(\bar{X}_2 - \bar{X}_1\right) + (R_2 - R_3) \left(\bar{X}_3 - \bar{X}_2\right) + (R_3 - R_1) \left(\bar{X}_1 - \bar{X}_3\right). \tag{57}$$

Then, a coin is flipped to determinate whether the exchange student is accepted or not. If so, a student is arbitrarily chosen from the population or abandoned.

The flowchart of MCTLBO is shown in Figure 5.

5.4. Application of MCTLBO

The system data, constraints, number of students or population size, maximum number of iterations, number of design variables or subjects (courses) offered coincide with the location of CSs with PV and BESS, number of PV panels, and number of BESSs to be placed in the IEEE 69-bus RDS. The constraints regarding placement of CSs with PV and BESS, limits of the number of PV, and limits of number of BESS are considered as the upper and lower limits of decision variables. The number of teachers here represents the number of objective functions considered simultaneously. CSs' placement buses, number of PV panels, and number BESS are positive integers. The decision variables are randomly generated and normalized between the maximum and minimum operating limits [20]. The implementation procedure of the MCTLBO algorithm to solve the problem is described in the flowchart, shown in Figure 5.

A full overview of the proposed methodology is shown in Figure 6.

6. Simulation and result analysis

The 69-bus RDS was divided into 6 zones using Eq. (15). Each zone is made up of load buses depending on the traffic network of the city. The details of assigning different load buses to different zones are given in Table 3 [2]. From each zone, one optimal location for CS is to be selected where PV and BESS units are to be placed, as shown in Figure 7.

The proposed MCTLBO optimization technique was tested in 69-bus RDS. The parameters of MCTLBO used in simulation were number of teachers = 2, maximum number of iteration = 150 and population size = 50. The results obtained from MCTLBO are compared with those obtained from NSGA-II. The parameters of NSGA-II used in the simulation were crossover distribution index (μ_c) = 20, mutation distribution index (μ_m) = 20, crossover probability (ρ_c) = 0.9, and mutation probability (ρ_m) = $\frac{1}{n}$, where n is the number of decision variables [20]. Maximum number of iterations and population size for NSGA-II were 150 and 50, respectively. The proposed algorithm for planning of CSs combined with PV and BESS was applied at 0.9 leading power factor. Power flow calculations were performed using base value 100 MVA and 12.66 kV [2]. The load bus was considered as the location for CSs; PV and BESS were placed in the same locations. The bus voltage is limited within the range of 0.95 p.u. to 1.05 p.u. The variables (location of CSs with PV and BESS, number of PV, and number of BESSs) with optimal compromised solutions are given in Table 4 and the convergence characteristics of the objective functions in both MCTLBO and NSGA-II are given in Figure 8. The compromised objective function values for only CS and CS with PV and BESS are given in Table 4. In addition, Table 4 illustrates the results obtained from the MCTLBO and compares them with that from NSGA-II. The superiority of the results from MCTLBO over the other method is observed.

The cost benefits of optimal placement of CSs with PV and BESS in RDS are given in Table 5. From Table 5, it is observed that CSs got an annual benefit of 23398226 INR after installation of PV and BESS.

The voltage profile of 69-bus RDS for all buses is shown in Figure 9. It can be observed that the presence of CSs for recharging EVs can significantly lower the bus voltages. The voltage profile can be improved by installing PV and BESSs at the CSs.

Figure 10 shows the voltage profile of bus 65.

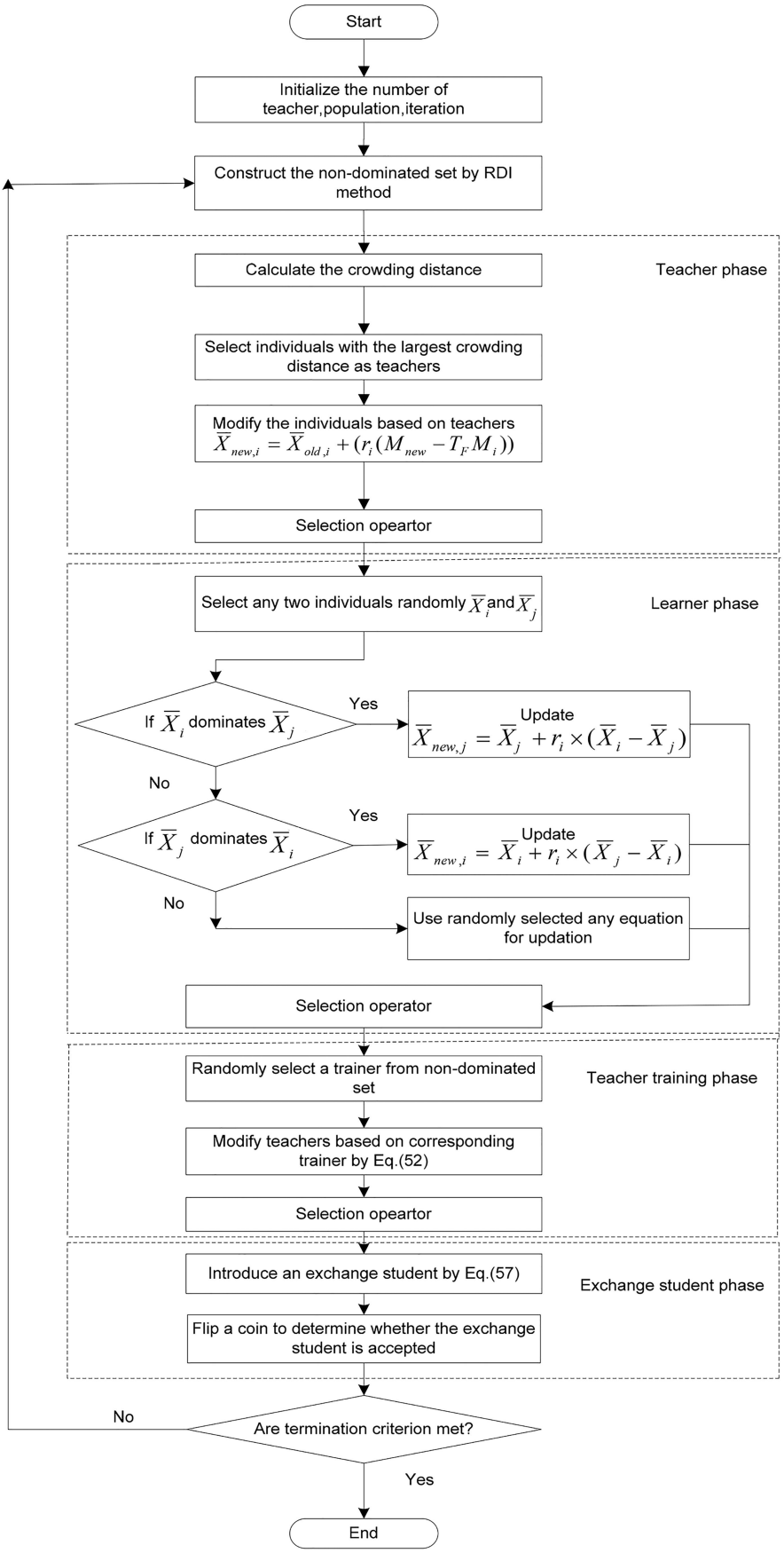

Figure 5. The flowchart of MCTLBO algorithm [39,40].

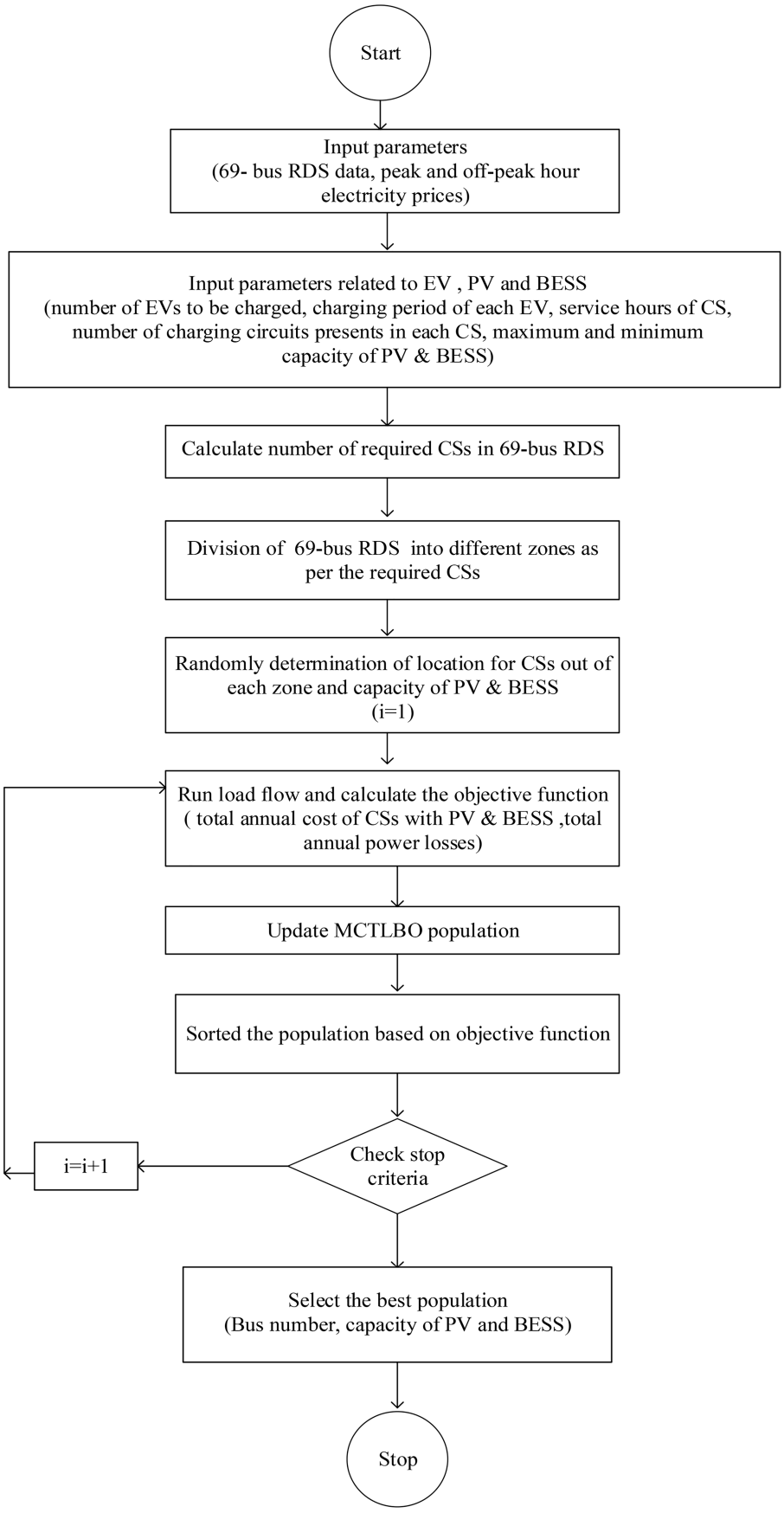

Figure 6. Flowchart of optimal sizing and location of PV/BESS and CSs.

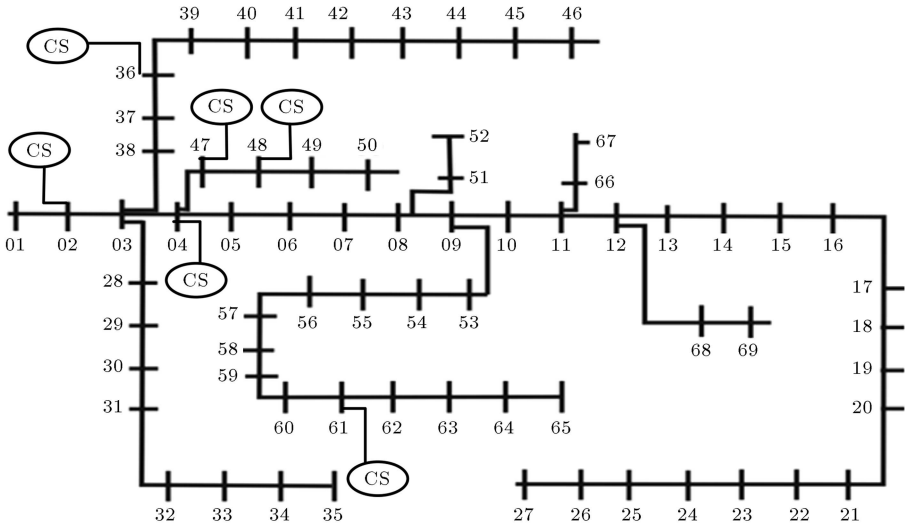

Figure 7. IEEE 69-bus RDS with 6 CSs.

Table 3. Specification of bus number in each zone of 69-bus RDS [2].

Zone	Bus no.
1	2, 5, 6, 9, 10, 13, 14, 17, 18, 22, 26, 31, 35
2	4, 7, 8, 11, 12, 15, 16, 19, 20, 23
3	27, 32, 36, 40, 45
4	21, 24, 25, 28, 29, 30, 33, 34, 37, 38, 39, 41, 42, 43, 46, 47, 49,51, 53
5	44, 48, 50, 52, 54, 58, 60, 62, 64
6	55, 57, 59, 61, 63, 65, 66, 67, 68, 69

Table 4. Multi-objective optimization results.

		Only CS		CS with PV and BESS	
		NSGA-II	MCTLBO	NSGA-II	MCTLBO
Charging station Location	CS 1	5	2	5	2
	CS 2	7	4	7	4
	CS 3	36	36	36	36
	CS 4	47	47	47	47
	CS 5	48	48	48	48
	CS 6	61	61	61	61
Number of PV		–	–	308, 304, 555, 306, 440, 869	302, 300, 300, 300, 304, 991
Number of BESS		–	–	246, 261, 263, 245, 251, 258	200, 203, 200, 200, 200, 200
Total cost (INR/year)		2685622	2682959	87526494	75908263
Total power loss (kW/year)		1505538	1385293	782416	716994
Voltage stability index (p.u.) of weakest bus		1.3884	1.3726	1.2268	1.2090

Table 5. Cost benefit analysis of CS.

$C_{grid,CS}$ (INR/year)	$C_{grid,CS}^{PV\&BESS}$ (INR/year)	$C_{grid,PV\&BESS}^{CS}$ (INR/year)	$C_{PV\&BESS}$ (INR/year)	Benefit (INR/year)
103075635	48443895	41991790	73225304	23398226

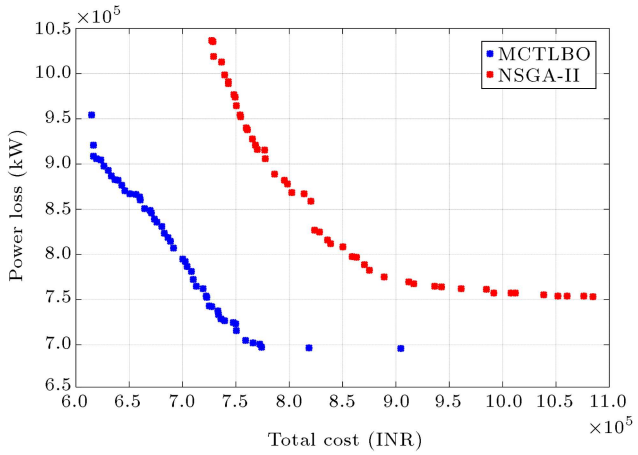

Figure 8. Variation of objective functions ($f_{obj,1}$, $f_{obj,2}$).

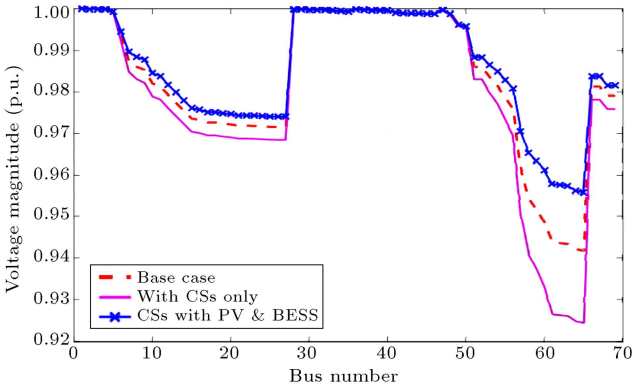

Figure 9. Voltage profile of 69-bus RDS in a day.

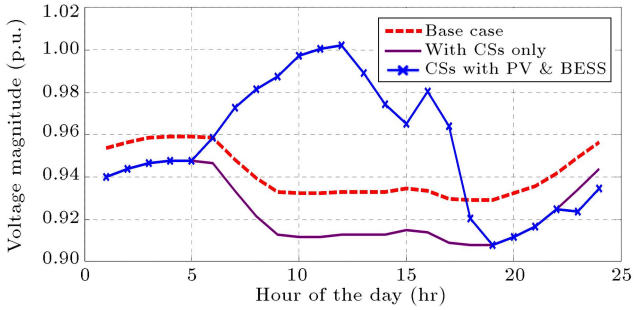

Figure 10. Voltage profile of 65-bus RDS in a day.

Given that the voltage level of this load bus is the lowest in the 69-bus system, its voltage profile is chosen for illustration. Before installation of PV and BESS, the voltage level of bus 65 was highly affected due to the presence of CSs only. Installation of PV and BESS with CSs enhances the hourly voltage profile of that bus.

Figure 11 shows the variation of active power loss in a day. Considerable improvements in terms of power loss reduction are obtained after the installation of CSs with PV and BESS. As per the adopted energy management strategy, during peak hour, the power drawn from the utility grid was lower than that at off-peak hour, as the electricity price is high during this period. This enables the CS to earn some revenues.

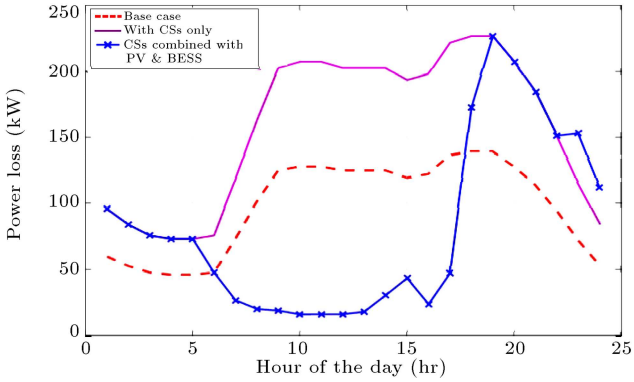

Figure 11. Variation of power loss in a day.

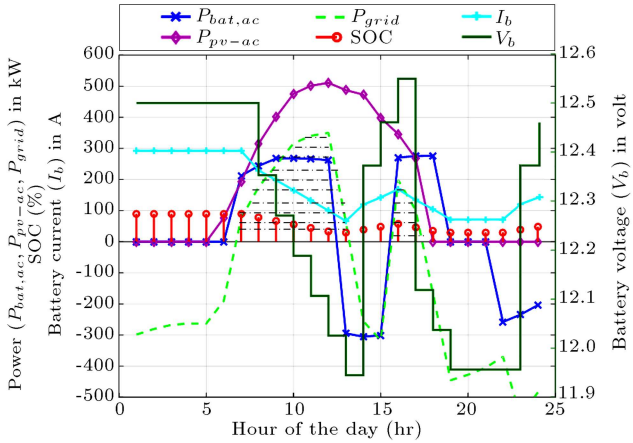

Figure 12. Variation of active power of PV, BESS, grid, SOC, battery voltage, and current in a day at bus 2.

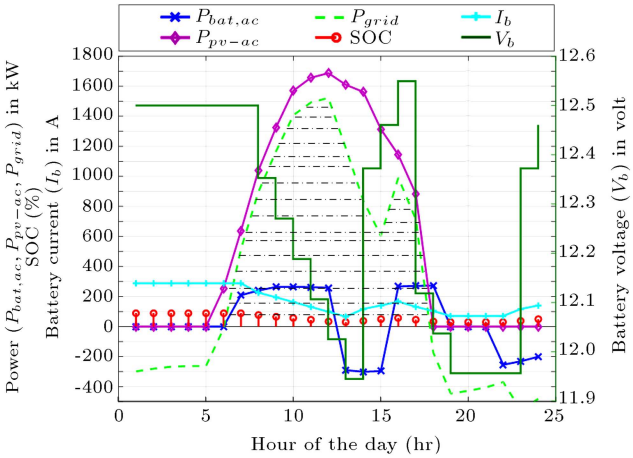

Figure 13. Variation of active power of PV, BESS, grid, SOC, battery voltage, and current in a day at bus 61.

Active power variations of PV, BESS, and grid for one day, SOC, battery voltage, and current in optimal locations of 2 and 61 are shown in Figures 12 and 13, respectively. The nature of the curves in the remaining optimal locations is more or less similar to bus 2, since

the sizes of PV panels and the BESSs in these locations are very close to those applied to bus 2. The BESSs are discharged during peak hours and charged during off-peak hours to alleviate upstream congestion by supplying downstream, distribution upgrade deferral, demand charge management, renewable energy time shift, and renewable capacity firming. During peak hour, the grid's demand at the selected bus and the CSs' demand are met by the PV and BESS.

The same type of BESS was used in CSs. Therefore, the SOC curves are the same. The BESS remains idle from the start of the day to 7 a.m. as it has maximum charge. After 7 a.m., following the beginning of the peak hour, the BES discharges until 1 p.m. Then, it charges during off-peak hours until 4 p.m. After 4 p.m., the BES again starts discharging until 7 p.m. during the evening peak hour and reaches the minimum SOC of 30%. Then, it remains idle and again starts charging at 11 p.m. as the off-peak hour starts.

From the start of the day, battery voltage remains at 12.5 V as the initial battery voltage. When BESS starts discharging, the minimum battery voltage is maintained at 11.94 Vand then, again increases during the charging periods. It is evident from battery current. The shaded part of the curves in Figures 12 and 13 denotes the amount of power sold to the utility grid. During these hours, the BESS sells the excess stored energy to the grid to make a benefit financially. By selling this power, the CS earns the benefit which in turn reduces the burden of electricity cost.

Figure 14 shows the 24-hour load demand profile for three cases, e.g., (i) base case, i.e., without EV charging stations, PV and BESS; (ii) with only EV charging stations; and (iii) with EV charging stations, PV, and BESS. In case (ii), with the inclusion of a large number of EVs, the load demand swells up to a great extent. However, the introduction of PV panels with BESS drags the load profile down even below that of the base case. In particular, during peak hours in the presence of sunlight, there is a significant

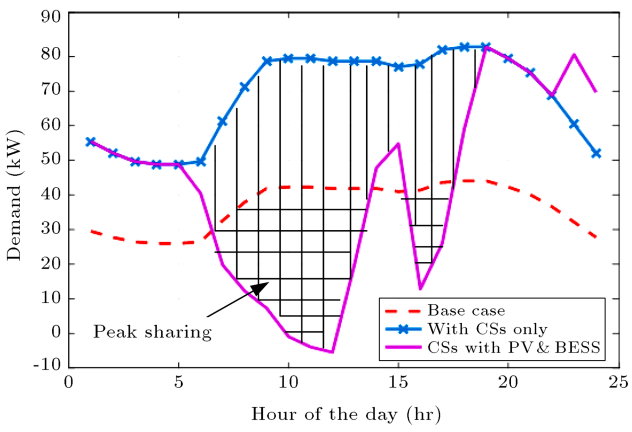

Figure 14. Hourly variation of load demand in kW.

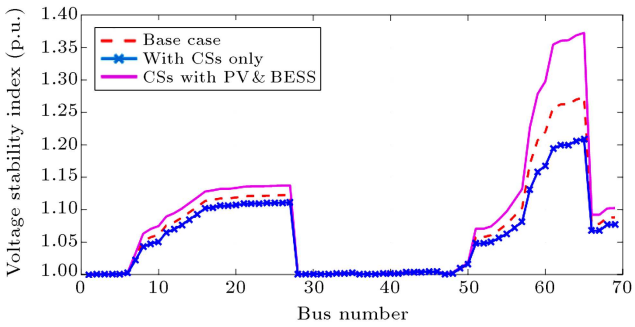

Figure 15. Voltage stability index in p.u. with CSs only and with CSs and PV/BESS for a 69-bus RDS.

load reduction. A spike in load demand in case (iii) results from BESS charging during the off-peak hours. Thus, according to Figure 14, introduction of PV and BESS facilitates peak load shaving and diverts the dependence of loads on the utility grid. It may agree with the network up-gradation deferral.

Figure 15 gives the voltage stability index of the IEEE-69 bus RDS for the three cases: (i) base case, i.e., without EV charging stations, PV, and BESS; (ii) with only EV charging stations; and (iii) with EV charging stations, PV, and BESS. The results show that the voltage stability index at the weakest bus is the lowest for the case of the inclusion of EV charging stations, PV, and BESS in comparison to cases (i) and (ii), because the PV/BESS injects reactive power at 0.9 leading power factor into the load bus, thus restricting the voltage from deviating much off the nominal value.

7. Conclusion

Based on the concept of sharing economy, this paper proposed a two-stage planning and operational architecture for the electricity grid to determine the optimal placement and sizing for distributed Photovoltaic (PV), Battery Energy Storage System (BESS), and Electric Vehicle (EV) charging stations. In the first case, Multi-Course Teaching Learning-Based multi-objective Optimization (MCTLBO) algorithm was employed to determine the optimal placement of EV charging stations' distribution on 6 zones of the network considering traffic conditions. Then, its impacts on the distribution system performances were analyzed. The corresponding optimal sizing of PV panels and BESS was realized at the second stage, where the Time Of Use (TOU) pricing model was applied to a 69-bus test system. The multi-objective functions consisted of total annual cost of Charging Stations (CSs) with PV and BESS as well as the total annual power loss in the network calculated in both of the cases considering system operational constraints. The effectiveness of installing PV panels and BESS was examined in this paper and it was proved to be an

economic supplement resource for the utility grid and charging station according to the simulation results. Moreover, this paper proposed a collectively shared BESS as a novel concept, which helps adapt more PV and BESS with the system. The result showed that this method was technically and economically feasible, while the optimal size of PV and BESS both increased to some extent in the test system.

The future works concern pricing, economic analysis, and optimal operational management for the services of 'cloud storage'.

Nomenclature

η_{pv}	PV generator reference efficiency (=15%)
A_{pv}	Area of the PV panel (= 33 m^2)
η_{pt}	Efficiency of perfect maximum power point tracker (= 100%)
I	Solar radiation
N_{pv}	Number of PV panels
f_{man}	De-rating factor for manufacture tolerance (= 97%)
f_{dirt}	De-rating due to dirt (= 95%)
η_{pv_inv}	Cable loss between the panel and inverter (= 97%)
T_{co}	Temperature coefficient (= 0.005)
T_{ref}	Reference temperature (= 25°C)
NOC	Nominal Operating Cell temperature (= 47.6°C)
T_{amb}	Ambient temperature (= 27°C)
η_{inv}	Inverter efficiency (= 97%)
η_{inv_sb}	De-rating due to AC cable loss (= 99%)
C	Ampere-hours that may be charged or discharged in 10 h at 25°C
I_b	Battery current during charging or discharging
I_{rate}	Charge or discharge current in 10 h at 25°C
V_b	Battery voltage
n_b	Number of cells in the battery (= 6)
ΔT	Temperature variation from reference of 25°C
E_{bat}	Stored energy in the battery (kWh)
w_h	Hourly weight factor
P_i	Peak load at the ith bus of RDS
$C_{CS,i}$	Capacity of charging station at the ith bus
NEV	Number of EVs to be charged in a day (= 3,140)
chg_{time}	Charging period of each EV (= 0.1667 hour)
s_h	Service hours of CS (= 24 hour)
q	Number of charging circuits present in each CS
n^{CS}	Number of required CSs in 69-bus RDS
$P_{Load,i}$	Predicted load demand of RDS at the ith bus
$P_{CS,i}$	Predicted load demand CS at the ith bus
$P_{dc,bat}$	BESS charging/discharging rate of the battery
$P_{bat,ac}$	BESS ac output at the AC bus bar
$C_{\max}$	Maximum capacity of the battery
C_{bat}	Capacity of the BES system
P_{pv_dc}	PV ac output at the AC bus bar
P_{pv_ac}	PV panel dc power output
P_{grid}	Active power delivered by the grid
Q_{grid}	Reactive power consumed by the grid
pf	Power factor of PV and BESS
C_{CS}	Total annual cost of CS
$C_{PV\&BESS}$	Total annual cost of PV and BESS
C_{INV}^{CS}	Annual investment cost
U_{INV}^{CS}	Investment cost of CSs that includes cost of all devices used and land cost for CS (= INR 20,51,100)
ir	Interest rate (= 10%)
e	Investment period (= 20 years)
$C_{O\&M}^{CS}$	Annual operational and maintenance cost of CS includes material cost, staff salary, maintenance and operation cost, and power consumption cost
σ	Conversion coefficient (= 0.12)
C_{TRV}^{CS}	Travelling cost of EVs used to calculate the total annual travelling of EVs to CSs to recharge the battery
x	Road twist coefficient (= 1.1)
ς	Smooth traffic coefficient of the road (= 1.1)
η	Turnaround coefficient (= 1.5)
k	Annual charging time of each EV (= 180)
l	Loss coefficient (= 1.3)
lp	Total number of load points (= 28)
g^{ph}	Service parameter for the pth EV load point of the hth CS whether the EV load point selects respective CS as a candidate station

d^{ph}	Distance between respective EV load point and CS in meter
C_{ele}^{CS}	Cost of electricity
E_{price}	Electricity price in INR/kWh
E_{grid}	Energy transfer to or from the utility grid in kWh
$d^{\max}$	Maximum distance between CS and load point of EV in kilometre (= 1.2 km)
$f_{INV}^{PV\&BESS}$	Annual investment cost of PV and BESS
$f_{INV}^{O\&M}$	Annual operational and maintenance cost of PV and BESS
$n^{PV\&BESS}$	Number of PV and BESS
$U_{INV}^{PV\&BESS}$	Investment cost of PV and BESS
ij	Branch number
R_{ij}	Resistance of the ijth branch
X_{ij}	Reactance of the ijth branch
I_{ij}	Current at the ijth branch
$P_{Loss,ij}$	Power loss of the ijth branch
P_{sub}	Active power injection by substation
Q_{sub}	Reactive power injection by substation
V_i	Voltage of the ith bus
$V_i^{\min}$	Minimum voltage of the ith bus
$V_i^{\max}$	Maximum voltage of the ith bus
$V_{i,nom}$	Nominal voltage of the ith bus (= 1 p.u.)
$I_{ij}^{\max}$	Maximum current at the ijth branch
$P_{pv\_dc}^{\min}$	Minimum dc output power of the PV panel
$P_{pv\_dc}^{\max}$	Maximum dc output power of the PV panel
$P_{dc,bat}^{\min}$	Minimum dc output power of the battery
$P_{dc,bat}^{\max}$	Maximum dc output power of the battery
$P_{EV}^{\min}$	Minimum charging capacity of EV
$P_{Ev}^{\max}$	Maximum charging capacity of EV
$P_{CS}^{\max}$	Maximum capacity of CS
P_h	Rated power output of charging circuit of CS
n_{EV}^{p}	Number of EVs at the pth EV load point
n_t	Time slot for one day (= 24 hrs)
d_{CS}	Distance between two adjacent CSs
$d_{CS}^{\max}$	Maximum distance limit in kilometre of two adjacent CSs as 3.0 km
$d_{CS}^{\min}$	Minimum distance limit in kilometre of two adjacent CSs as 0.15 km
B_{CS}	Cost benefits of CSs installing with PV and BESS
$C_{grid,CS}$	Cost of power drawn from the grid by only CS
$E_{grid,CS}$	Power drawn from grid by only CS
$C_{grid,CS}^{PV\&BESS}$	Cost of power consumed from the grid by CS after installation of PV and BESS
$E_{grid,CS}^{PV\&BESS}$	Power consumed from the grid by CS after installation of PV and BESS
$C_{grid,PV\&BESS}^{CS}$	Cost of power delivered to grid by PV and BESS installed at CS
$E_{grid,PV\&BESS}^{CS}$	Power delivered to grid by PV and BESS installed at CS
M_i	Mean of the class in iteration i
M_{new}	Current teacher
T_F	Teaching factor
r_i	Random number in (0, 1)
P_j	Active load at the jth receiving bus
Q_j	Reactive load at the jth receiving bus
$\|f(\bar{X})\|$	Objective function vector norm

References

1. Wirges, J., Linder, S., and Kessler, A. "Modelling the development of a regional charging infrastructure for electric vehicles in time and space", *Eur. J. Transp. Infrast.*, **12**(12), pp. 391–416 (2012).
2. Kasturi, K. and Nayak, M.R. "Optimal planning of charging station for EVs with PV-BES unit in distribution system using WOA", *IEEE Int. Conference on Man and Machine Interfacing* (2017).
3. Vliet, O., Brouwer, A.S., Kuramochi, T., et al. "Energy use, cost and CO2 emissions of electric cars", *J. Power Sources*, **196**(4), pp. 2298–2310 (2011).
4. Mullan, J., Harries, D., Braunl, T., et al. "Modelling the impacts of electric vehicle recharging on the Western Australian electricity supply system", *Energ. Policy*, **39**(7), pp. 4349–4359 (2011).
5. Bossche, P.V.D., *CHAPTER TWENTY-Electric vehicle charging infrastructure, electric and hybrid Vehicles*, Elsevier, Amsterdam, pp. 517–543 (2010).
6. Wei-dong, X. and Wei, L. "Modelling and simulation of public EV charging station with power storage system", *Int. Conf. on Electric Info. and Control Engg. (ICEICE)*, pp. 2346–2350 (2011).
7. Pazouki, S., Mohsenzadeh, A., and Haghifam, M.R. "Optimal planning of PEVs charging stations and demand response programs considering distribution and traffic networks", *IEEE Smart Grid Conf.*, pp. 90–95 (2013).

8. Phokornchai, P. and Leeprechanon, N. "Multiobjective optimal placement of public fast charging station on power distribution network using hybrid ant colony optimization and bees algorithm", *Int. J. of Engg. and Tech.*, **8**, pp. 2431–2442 (2017).
9. Zhipeng, L., Fushuan, W., and Ledwich, G. "Optimal planning of electric-vehicle charging stations in distribution system", *IEEE T. Power Deliver*, **28**, pp. 102–110 (2013).
10. Jamian, J.J., Mustafa, M.W., Mokhils, H., et al. "Minimization of power losses in distribution system via sequential placement of distributed generation and charging station", *Arab. J. Sci. Eng.*, **39**(4), pp. 3023–3031 (2014).
11. Moradi, M.H., Abedini , M., Reza Tousi, S.M., et al. "Optimal siting and sizing of renewable energy and charging stations simultaneously based on differential evolution algorithm", *Elect. Power and Energy Sys.*, **73**, pp. 1015–1024 (2015).
12. Aksanli, B. and Rosling, T. "Optimal battery configuration in a residential home with time of use pricing", *IEEE Int. Conf. on Smart grid Com.* (2013).
13. Sfikas, E.E., Katsigiannis, Y.A., and Georgilaki, P.S. "Simultaneous capacity optimization of distributed generation and storage in medium voltage microgrid", *Elect. Power and Energy Sys.*, **67**, pp. 101–113 (2015).
14. Amini, M.H., Moghaddam, M.P., and Karabasoglu, O. "Simultaneous allocation of electric vehicles' parking lots and distributed renewable resources in smart power distribution networks", *Sustain. Cities Soc.*, **28**, pp. 332–342 (2017).
15. Bahrami, S. and Parniani, M. "Game theoretic based charging strategy for plug-in hybrid electric vehicles", *IEEE T. Smart Grid*, **5**(5), pp. 2368–2375 (2014).
16. Mozafar, M.R., Moradi, M.H., and Amini, M.H. "A simultaneous approach for optimal allocation of renewable energy sources and electric vehicle charging stations in smart grids based on improved GA-PSO algorithm", *Sustain. Cities Soc.*, **32**, pp. 627–637 (2017).
17. Mohammadi, A., Mehrtash, M., and Kargarian, A. "Diagonal quadratic approximation for decentralized collaborative TSO+ DSO optimal power flow", *IEEE Transactions on Smart Grid*, **10**(3), pp. 2358–2370 (2018).
18. Bahrami, S. and Wong, V.W. "A potential game framework for charging PHEVs in smart grid", In *Comm., Comp. and Signal Pro., IEEE Pacific Rim Conference on IEEE*, pp. 28–33 (2015).
19. Bahrami, S., Wong, V.W., and Huang, J. "An online learning algorithm for demand response in smart grid", *IEEE T. Smart Grid*, **9**(5), pp. 4712–4725 (2018).
20. Kasturi, K. and Nayak, M.R. "Multi-objective MCTLBO approach to allocate renewable energy system (PV/BESS) in electricity grid: assessing grid benefits", *Int. J. Energ. Techno. & Polices*, **16**(1), pp. 1–23 (2020).
21. RTS Task Force: The IEEE reliability test system-1996", *IEEE Trans. Power Syst.*, **14**(3), pp. 1010–1020 (1999).
22. Nayak, M.R. and Nayak, C.K. "Distributed generation optimal placement and sizing to enhance power distribution network performance using MTLBO", *Int. Rev. Electr. Eng.-I*, **6**, pp. 1857–1869 (2013).
23. Kanzumba, K. "Optimal scheduled power flow for distributed photovoltaic/wind/diesel generators with battery storage system", *IET Renew. Power Gen.*, pp. 1–9 (2015).
24. "Clean Energy Council, *Grid-Connected Solar PV Systems (No Battery Storage) Design Guidelines For Accredited Installers* (2013). Available: www.solaraccreditation.com
25. Shi, Z., Wang, R., Zhang, X., et al. "Optimal design of grid-connected hybrid renewable energy systems using multi-objective evolutionary algorithm", *Sci. Iran. Trans. D.*, **24**(6), pp. 3148–3156 (2017).
26. Indian Meteorological Department, Bhubaneswar, India (2015). www.imd.gov.in
27. Lujano-Rojas, J.M., Dufo-Lopez, R., and Bernal-Agustin, J.L. "Optimal sizing of a small wind/battery systems considering the DC bus voltage stability effect on energy capture, wind speed variability and load uncertainty", *Appl. Energ.*, **93**, pp. 404–412 (2012).
28. Wang, W., Chengxiong, M., Lu, J., et al. "An energy storage system sizing method for wind power integration", *Energies*, **6**, pp. 3392–3404 (2013).
29. Nayak, C.K. and Nayak, M.R. "Optimal design of battery energy storage system for peak load shaving and time of use pricing", *Int. Conf. Elect. Comp. and Comm. Tech.* (2017).
30. Copetti, J. and Chenlo, F. "Lead/acid batteries for photovoltaic applications. Test results and modelling", *J. Power Sources*, **47**(1–2), pp. 109–118 (1994).
31. Nayak, C.K. and Nayak, M.R. "Technoeconomic analysis of a grid-connected PV and battery energy storage system considering time of use pricing", *Turk. J. Electr. Eng. Co.*, **26**(1), pp. 318–329 (2018).
32. Lambert, T., *Battery Roundtrip Efficiency*, HOMER Software, Help Index (2004).
33. Ton, D.T., Peek, G.H., Hanley, C.J., et al. "Solar energy grid integration systems - energy storage (SEGIS-GS)", EERE Publication and Product Library, Washington, DC (United States) (2008).
34. Leeprechanon, N., Phokornchai, P., and Sharma, M.K. "Optimal planning of public fast charging station on residential power distribution system", *Trans. Electrification Asia-Pacific (ITEC Asia-Pacific), IEEE Conf. and Expo.* (2016).
35. Nayak, C.K., Nayak, M.R. and Behera, R. "Simple moving average based capacity optimization for VRLA battery in PV power smoothing application using MCTLBO", *J. Energy Storage*, **17**, pp. 20–28 (2018).

36. Cheol, L.W., Choi, J.P., and Huynh, C.K. "A modified tone injection scheme for PAPR reduction using genetic algorithm", *ICT Express 1.2*, pp. 76–81 (2015).

37. Rao, R., Savsani, V., and Vakharia, D. "Teaching-learning-based optimization: A novel method for constrained mechanical design optimization problems", *Comput. Aided D.*, **43**(3), pp. 303–315 (2011).

38. Bhattacharjee, K., Bhattacharya, A., and Dey, S.H.N. "Teaching-learning-based optimization for different economic dispatch problems", *Sci. Iran. Trans. D.*, **21**(3), pp. 870–884 (2014).

39. Lin, W., Wang, L., Tian, G., et al. "MTLBO: A multi-objective multi-course teaching-learning-based optimization algorithm", *J. Appl. Sci. Eng.*, **21**, pp. 331–342 (2018).

40. Nayak, C.K., Nayak, M.R., and Behera, R. "Simple moving average based capacity optimization for VRLA battery in PV power smoothing application using MCTLBO", *J. Energ Storage*, **17**, pp. 20–28 (2018).

Biographies

Kumari Kasturi was born in 1986, India. She received her BTech degree in Electrical Engineering from Biju Patnaik University (BPUT), Odisha, India and MTech degree in Electrical and Electronic Engineering from I.T.E.R, SOA University, Odisha, India. Since 2008, she has been with Electrical Engineering Department, I.T.E.R, Siksha 'O' Anusandhan University, Bhubaneswar, Odisha, India-751030 and continuing as an Assistant Professor. She is recently awarded with her PhD from Siksha 'O' Anusandhan University, Odisha in 2020. Her research interests include power system operation and planning, distribution network, distributed generation and application of soft computing techniques to power system optimization. She has membership in IEEE society (ID No. 96584246).

Manas Ranjan Nayak was born in 1972, Odisha, India. He received his BE, ME, and PhD degree in Electrical Engineering in 1994, 1995, and 2014, respectively. He is presently continuing as an Associate Professor at the Department Electrical Engineering, Biju Patnaik University of Technology, Odisha, Rourkela, India-769015. His research interests include power system operation and planning, distributed renewable generation, energy storage system, electric vehicle integration, and application of soft computing techniques to power system optimization. Professor Nayak has membership in professional societies, i.e., IET (70472641) and ISTE (LM-71207)

Chinmay Kumar Nayak was born in 1988. He received his BE degree in Electrical and Electronics Engineering, M.I.T., Manipal (Manipal University, India) and MTech degree in Electrical Engineering with specialization in Energy Systems & Management from I.T.E.R, SOA University, Odisha, India in 2011 and 2013, respectively. He is currently continuing as a PhD scholar in Utkal University, India. His research interests include energy storage systems, energy system management, distributed renewable generation, evolutionary optimization techniques, and power system optimization.